A Review of Basic to Clinical Studies of Irreversible Electroporation Therapy

Chunlan Jiang, Rafael V. Davalos, *Member, IEEE*, and John C. Bischof*

***Abstract*—The use of irreversible electroporation (IRE) for cancer treatment has increased sharply over the past decade. As a nonthermal therapy, IRE offers several potential benefits over other focal therapies, which include 1) short treatment delivery time, 2) reduced collateral thermal injury, and 3) the ability to treat tumors adjacent to major blood vessels. These advantages have stimulated widespread interest in basic through clinical studies of IRE. For instance, many *in vitro* and *in vivo* studies now identify treatment planning protocols (IRE threshold, pulse parameters, etc.), electrode delivery (electrode design, placement, intraoperative imaging methods, etc.), injury evaluation (methods and timing), and treatment efficacy in different cancer models. Therefore, this study reviews the *in vitro*, translational, and clinical studies of IRE cancer therapy based on major experimental studies particularly within the past decade. Further, this study provides organized data and facts to assist further research, optimization, and clinical applications of IRE.**

***Index Terms*—Animal, clinical, enhancement, *in vitro*, irreversible electroporation (IRE).**

I. Introduction

ELECTROPORATION[1] is a technique that utilizes high-magnitude electric pulses (thousands of V/cm) to induce permeability increase in cell membranes. While some of the molecular events that take place at the membrane level have not been fully elucidated, there is general agreement in the literature [1], [2] that nanometer-sized metastable structural defects or "pores" are created when the plasma membrane is exposed to the external pulsed electric field. These pores are thought to be the source of the increased permeability from electroporation first used for material (i.e., DNA, protein, etc.) transfer into cells and then later as a therapeutic modality to treat diseases as reviewed below.

Manuscript received May 19, 2014; revised September 6, 2014 and October 23, 2014; accepted October 23, 2014. Date of publication November 6, 2014; date of current version December 18, 2014. This work was supported in part by Ethicon Endo-Surgery, Inc. The work of R. Davalos was supported by NSF CAREER Award CBET-1055913. The work of J. C. Bischof was supported in part by the Carl and Janet Kuhrmeyer Chair in Mechanical Engineering at UMN. *Asterisk indicates corresponding author.*

C. Jiang is with the Mechanical Engineering Department, University of Minnesota, Minneapolis, MN 55455 USA (e-mail: jiang240@umn.edu).

R. V. Davalos is with the Virginia Tech-Wake Forest School of Biomedical Engineering and Sciences, Bioelectromechanical Systems Laboratory,Virginia Polytechnic and State University, Blacksburg, VA 24061 USA (e-mail: davalos@vt.edu).

*J. C. Bischof is with the Mechanical and Biomedical Engineering Departments, University of Minnesota, Minneapolis, MN 55455 USA (e-mail: bischof@umn.edu).

Color versions of one or more of the figures in this paper are available online at http://ieeexplore.ieee.org.

Digital Object Identifier 10.1109/TBME.2014.2367543

[1]A variety of terminology, such as electropermeabilization, has been used to refer to the physics of this phenomenon.

The first observation of electroporation was reported in the 1950s on electrically stimulated membranes [3] and was described as "membrane breakdown," which in more recent work is considered to be an increase of membrane conductance or permeability. Soon thereafter, the nonthermal killing effects of strong electric field pulses were discovered and reported by Sale in a study on microorganisms [4]. Many studies followed into the early 1990s demonstrating the utility of electroporation in molecular biology, mainly as a method to introduce foreign molecules into living cells when electroporation is reversible. Although further exploration and optimization for cancer continue, reversible electroporation has been used for decades for molecular and gene transfer *in vitro* [5]–[7].

The introduction of electroporation to cancer therapy originated from drug delivery applications. Specifically, electroporation was used to assist uptake of chemotherapeutic drug molecules into tumor cells [8]. The pairing of electroporation and chemotheapeutic drug quickly gained popularity and now exists as an independent treatment termed electrochemotherapy (ECT) which is in clinical practice [9]–[11]. The reported objective response rates of ECT range from 72% to 100% [12], [13] and is one of the most well-established clinical applications of electroporation today [14].

In 2005, the concept of using electroporation as a monotherapy (i.e., without cytotoxic drugs or in conjunction with thermal effects) to destroy tissue was proposed by Davalos *et al.* [15]. The term "irreversible electroporation (IRE)" was used to distinguish between cell destruction rather than reversible permeabilization used in previous embodiments of electroporation for molecular biology applications. In this study, IRE alone showed the ability to destroy undesirable tissues in the body in a manner similar to more traditional focal thermal therapies such as radiofrequency (RF) heating or cryosurgery. The advantages over thermal therapies were immediately realized due to IRE's potential to: 1) reduce treatment time, 2) reduce collateral thermal effects (i.e., overtreatment), and 3) avoid influence of local blood perfusion on treatment outcome (i.e., no blood sink or source to heat transfer). These advantages quickly triggered widespread interest from the scientific community leading to many studies both *in vitro* [16]–[19] and *in vivo* [20]–[24]. Further, a wide variety of cell [16]–[19], organ [25]–[27], and animal [20], [23], [28] models have been used to characterize the destructive potential of IRE for different cancer types.

These studies have provided valuable experimental results and treatment planning protocols (IRE threshold, pulse parameters, etc.) including electrode delivery (electrode design, placement, intraoperative imaging methods, etc.), injury evaluation (methods and timing), and treatment efficacy. While reviews of

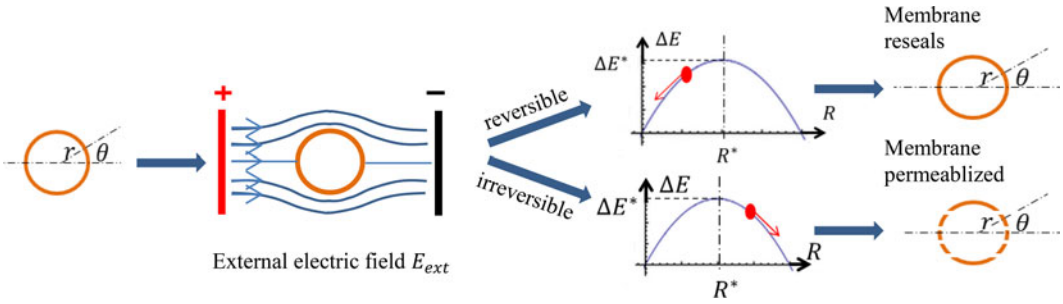

Fig. 1. Illustration of electroporation process and outcome [29], [30]. ΔE is the free energy to create a pore of radius R.

IRE are now beginning to be published [1], [2], [31]–[35], a summary and categorization of basic to clinical IRE studies allowing ready access and comparison between protocols and parameters has not yet been provided for researchers and clinicians who are new to the field or would like a more comprehensive reference.

Therefore, the main purpose of this study is to critically review the *in vitro,* translational, and clinical work based on major experimental studies on IRE therapy in the past decade, and provide organized data and facts to assist further research, optimization, and clinical applications with IRE.

II. Proposed Mechanisms of IRE

A more complete treatment of this topic can be found in many reviews of the subject [29], [33], [36]–[39]. However, for completeness and later discussion, a brief overview of mechanisms is given here.

Electroporation is essentially a membrane phenomenon that involves behavior of the lipid plasma membrane under the intense stimulation of external electric field. The early observation of electroporation dates back more than half a century ago [3]. However, it was not until the 1970s that insights into IRE mechanisms began to accumulate with the development of experimental platforms. Using a natural vesicular membrane system, Neumann and Rosenheck [40] detected the release of catecholamines induced by intense electric field and confirmed the transient change of membrane permeability during electroporation. In a subsequent series of studies [41]–[46], it was suggested that the site of interaction between the electric field and the cell subjects was the cell membrane. These findings stimulated great interest in modeling the membrane lipid system and developing membrane-based mechanisms for electroporation.

The potential distribution surrounding an isolated spherical cell (see Fig. 1) [30] with a nonconducting membrane in an external electric field E_{ext} can be described by Laplace equation and has the following solution for the transmembrane voltage (U):

$$U = f \cdot r \cdot E_{\text{ext}} \cdot \cos\theta \cdot \left(1 - e^{-\frac{t}{\tau}}\right)$$
$$\text{where } \tau = r \cdot C_m \cdot \left(\frac{1}{\sigma_i} + \frac{1}{2\sigma_e}\right) \tag{1}$$

where r is the radius of the cell, and θ is the angle between the site on the cell membrane where U is measured and the direction of E_{ext}, f (mV/(V/cm)) is a coefficient introduced to reflect the influence of cell packing density, i.e., the ratio of cell radius to cell separation distance, and the membrane charging time constant τ_c determined by C_m (specific membrane capacitance), σ_i and σ_e (intracellular and extracellular specific conductivities) [36], [47]–[50]. Following this approximation, for a typical eukaryotic cell with a radius of $r = 10\ \mu\text{m}$, it takes a field strength of 667 V/cm to achieve a transmembrane voltage of 1 V [29]. It should be noted that (1) holds true just prior to the onset of electroporation. As noted by DeBruin and Krassowska [50], the potential drop across the membrane dampens at the poles at the onset of electroporation. Three papers by Kinosita are pioneering demonstrations of some basic features of electroporation [51]–[53] and are almost entirely explained by the cell model of Krassowska and Filev [48]. Only the experimentally observed transmembrane voltage and underlying pore distribution asymmetry are not explained by this model.

There have been several different types of theoretical models explaining membrane stability at elevated transmembrane voltages. In earlier studies, it was suggested that membrane rupture is caused by an electromechanical collapse due to the compression of the entire membrane [54]. However, according to this model, there is a deterministic threshold for each specific cell type, which is contradictory to the stochastic nature of IRE from experiments. Based on the earlier studies by Litster [55], [56] on stability of spontaneous pores on membranes, Weaver and Mintzer [57] proposed an energy-based pore formation model for membrane rupture during electroporation. In this model, the free energy for pore formation is dependent on both the membrane properties and the applied external electric field

$$\Delta E\,(R, U) = 2\pi R \cdot \lambda - \pi R^2 \cdot \left(\sigma + aU^2\right) \tag{2}$$

where $\Delta E\,(R, U)$ is the free energy to create a pore of radius R, λ and σ are the edge line tension and surface tension of the membrane, respectively, and a represents the contrast of dielectric constants of water and lipid. This model accounts for factors of both the applied external electric field and the membrane's intrinsic physical properties, such as line tension and surface tension, which could also influence the outcome of electroporation [58] (see Fig. 2). Furthermore, it allows for estimation of the pore formation rate with calculations described in [29], [59], and [60].

The mechanisms whereby cells die post IRE continue to be actively investigated. Several mechanisms with experimental

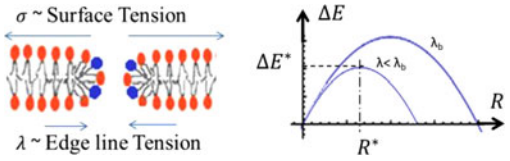

Fig. 2. Reported IRE influencing factors: (a) Competing factors (σ and λ) during pore formation. (b) Nucleation based energy model and critical pore radius & energy with baseline (λ_b) or decreased edge line tension ($\lambda < \lambda_b$).

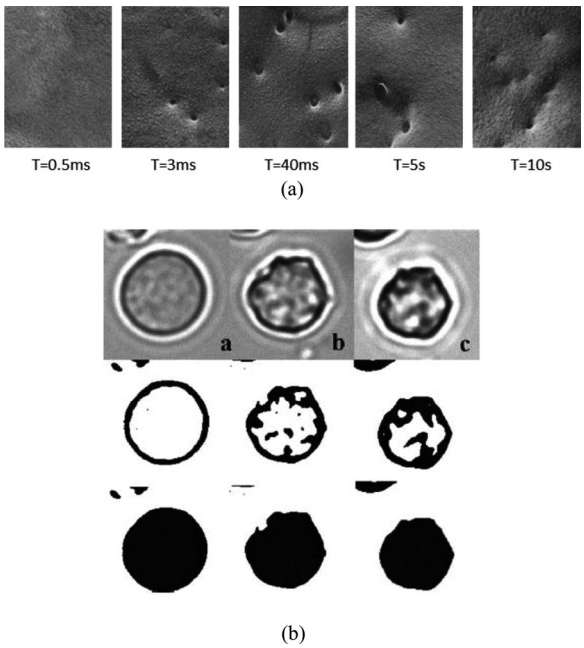

Fig. 3. Experimental observations of electroporation. (a) Observation of numerous "pore-like" structures from samples rapidly frozen after electroporation and then imaged by freeze fracture under the electron microscope [61]. (b) Volumetric response of cells during electroporation [66]. Reprinted with the permissions from Elsevier.

support have been proposed and are reviewed here. One mechanism is lethal membrane disruption from repetitive electrical pulsing. This lethal event is predicted in existing electroporation theories [1], [2], [29], [37], [59] considering the creation of aqueous pores. Direct visualization of the transient pore formation process has been elusive due to the combination of time scale and spatial resolution limit of the imaging methods. However, attempts based on "fix-then-process" approaches have been made to observe the membrane pore induced by electroporation. Using electron microscopy (EM), Chang and Reese [61] were able to observe "pore-like" structures from rapid frozen electroporation treated samples [see Fig. 3(a)]. Because direct poration is difficult to detect, researchers have often resorted to indirect measurements which may support either poration or permeabilization. For instance, sharp changes in electrical conductivity can reflect alteration of membrane permeability and can be used to detect the occurrence of electroporation [62]–[65]. Dye uptake and volumetric response of cells [see Fig. 3(b)] have also been used to evaluate pore formation during electroporation [16]–[18], [66]. In addition, for the nonvital pores that completely reseal after electroporation, many secondary events, such as electroconformational protein denaturation [36], osmotic imbalance, flush in/out of ions [67], depletion of adenosine triphosphate (ATP) [68], and uptake of toxic/foreign molecules [13], could occur before complete pore reseal and may eventually result in cell death. Numerous studies have reported the "delay" of injury development after electroporation [27], [68], [69]. ECT also takes advantage of the permeability change during electroporation to introduce cytotoxic drugs to kill cancer cells [70]. Studies have shown that the secondary events mentioned above could potentially cause more injury than primary membrane pore [68].

In summary, the current understanding of IRE is that it is linked to and occurs within the plasma membrane. There tends to be general agreement about the pore formation process although how the membrane recovers is poorly understood and an area of ongoing research [29], [32], [38], [71]. Two possible explanations of cell death are permanent membrane lysis or loss of homeostasis (i.e., loss of cellular contents prior to resealing).

III. *In Vitro* Studies of IRE

The majority of research on *in vitro* electroporation was conducted for molecular biology applications before IRE was proposed as a tissue destruction modality. The *in vitro* model systems were typically cell suspension in cuvettes and microfluidic channels that are also systems that have been studied for molecular biology applications, such as genetic transfection and *in vitro* drug testing. Nevertheless, the goal of most of these applications is to increase the uptake of desired molecules while minimizing cell injury (i.e., reversible electroporation). It is beyond the scope of this paper to include all of these results here although the interested reader can find numerous reviews in this area [7], [72], [73]. Thus, in this paper, only the studies with IRE (i.e., cell destruction) as the goal, or those that provided insights on electroporation mechanisms relevant to cell destruction are included.

A. *In Vitro Models*

The *in vitro* model systems for IRE that have been studied and published in literature can be classified into three categories based on the type of membrane studied [29], [71]. These categories include 1) artificial membrane systems, including lipid bilayer sheet membrane [74], [75] or vesicles [40], 2) isolated single cells [63], [76], and 3) cell suspension in cuvettes or microfluidic channels [16]–[19]. The artificial membrane models ignore the intercellular and intracellular structures and, therefore, cannot account for how these structures may affect cell death pathways. However, due to their simplicity, artificial membrane models are easy to manipulate and image and, therefore, have contributed to numerous insights at the membrane level, such as direct observation of membrane surface change and measurements of pore formation timing and size [40], [41], [43]–[45], [74]. Single-cell models isolate the individual cells from their extracellular environment and provide access for cell behavior by direct observation and measurements of electrical properties. Early experimental studies chose larger cells (e.g.,

muscle cells and oocytes) due to the ease of manipulation [63], [77], [78]. More recently, microfluidic devices allow researchers to conduct electroporation on smaller cells (tens of micrometer in diameter) using micropipette tips and microelectrodes [79]–[84]. The cell suspension model is the most widely used experimental system for *in vitro* cell destruction studies. It allows observation of a group of cells under external electrical stimulation. Here, membrane or extracellular properties can be adjusted by changing or adding components in the medium, allowing optimization of IRE conditions [16]–[18], [58]. Importantly, cell suspensions allow measurement of ensemble average behavior within a cell population, whereas individual cell behavior requires more specialized microfluidic or other platforms as already mentioned.

B. Electroporation Time Frame

The generation of transmembrane potentials that can affect IRE in a large lipid vesicle ($\sim$40 μm) or a single cell ($\sim$50 μm) typically happens on the order of microseconds [32], [50], [62], [85]. Once formed, pores in the lipid domain can last milliseconds to seconds after the external electric field is removed, as has been shown for bilayer lipid membranes or lipid vesicles [41]. Experimentally, the kinetics of membrane changes during electroporation have been monitored by permeability, conductivity, fluorescence imaging, and EM [51], [52], [61], [86]–[92]. Among the first recorded event is a pore initiation in the microsecond range that can be measured by permeability changes and confirmed by leakage experiment [89], [93]. Interestingly, these pores can persist for longer times. For instance, EM detects pore-like structures after 10 ms after pulse termination [61], and they lasted in some cases up to 10 s which was quite unexpected. Another EM study observed pore like structures at 15 min or even 24 h after IRE treatment in tissue [94]. One possible explanation is that EM is visualizing large pore-like imprints due to secondary effects during recovery rather than pores themselves [85].

Importantly, both theory and experiment indicate that electroporation induces membrane events within a membrane charging time that is less than microseconds. The amount of time it takes for a membrane to demonstrate pores from electroporation can range from microseconds to milliseconds. After the external electrical field is withdrawn, it may take the membrane seconds to hours to recover if immediate lethal injury has been avoided (see Fig. 4). Importantly, each of the time frames above depends strongly on the cell/membrane type and the applied electric field. Therefore, the time frame illustrated in Fig. 4 is only qualitative. It would be of great interest to find models that make quantitative predictions of the electroporation time frame for specific cell/membrane types.

C. Injury Mechanisms and Evaluation

As already mentioned, pore formation does not necessarily result in cell death. The critical cellular injury comes from either direct membrane destruction (irreversible pore, rupture, etc.) that deployed cytoskeleton (and/or extracellular matrix connection to the cell through proteins), or secondary effect such as

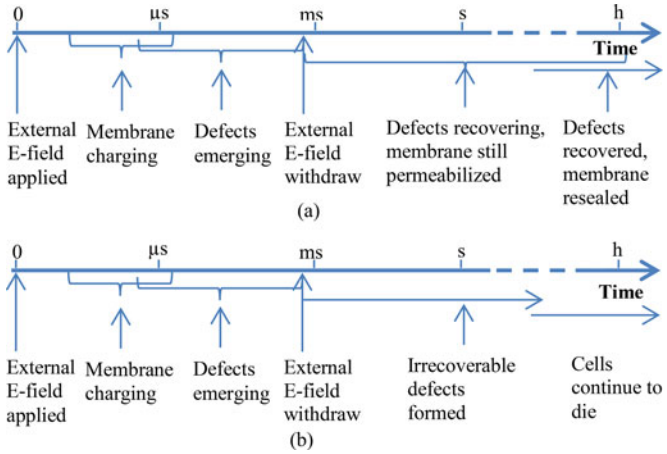

Fig. 4. Illustration of the time frames of (a) reversible and (b) irreversible electroporation.

osmolarity imbalance, loss of critical organelles, or influx of cytotoxic molecules that eventually result in cell death. Therefore, it is important to examine existing *in vitro* injury evaluation methods and discuss their advantages and disadvantages.

The classic membrane integrity dye assay (PI, Hoechst, Trypan blue, etc.) is simple, inexpensive, and detects direct membrane defects. However, several questions need to be carefully considered before using membrane integrity assays. First, when should the dye be introduced? This is important since it is possible that both reversible and irreversible pores are present in the membrane during IRE. So, if the dye is introduced before IRE, the "dead" cell count will be biased as cells with only reversible pores may eventually survive and yet will be counted as dead. On the other hand, if the dye is introduced after IRE, reversible pores may seal after dye entry into the cell after seconds to hours. One rule of thumb if dyes are used is to keep the time period (usually minutes) after loading constant and report it with their experimental results. Second, how long will the dye be incubated? This is important since after prolonged incubation, secondary injury from IRE will tend to increase cell death by dye count over time. The timing of such processes is unpredictable and may result in inconsistent viability if the waiting period is varied. Therefore, the timing of dye application and incubation time need to be carefully controlled and considered when comparing results obtained from one study to another using membrane integrity dye assays.

NAD(P)H-dependent cellular oxidoreductase enzymatic (MTT, XTT, CCK, etc.) assays are another class viability assays. These colorimetric assays measure the activity of cellular enzymes which reduce the tetrazolium based dyes via NAD(P)H-dependent metabolic activities, thereby reflecting the number of viable cells present. The advantage of this type of assay is that it can detect a dead (or dying) cell under conditions other assays cannot. For instance, the dye assay can only detect cell death when the membrane is compromised whereas NAD(P)H assay can detect cell death when it is still intact. However, NAD(P)H-dependent assay does not have the capability to differentiate between metabolically dormant and dead cells. In addition,

TABLE I
SUMMARY OF *In Vitro* IRE STUDIES

	Model	System	Electric Field (V/cm)	Pulse Parameters			Injury Evaluation[#]	Ref.
				Number	Duration (μs^)	Freq. (Hz)		
Cancer Cells	HepG2 (liver)	Cuvette	1500	30	300	0.1	a, c	[1]
	M109 (lung)	μChannel	300∼400	n/a	100∼300 ms	n/a[*]	a	[5]
	DC-3F (lung)	Cuvette	1200	8	99	n/s[*]	c, e	[4]
	Lewis (lung)	Cuvette	1400	8	99	n/s	c, e	[4]
	PC3 (prostate)	Cuvette	250∼2000	10∼3840	100 μs	10	a	[2]
	THP-1 (leukemia)	Cuvette	1500∼7500	1	2 or 5 ms	n/a	a	[3]
	K-562 (leukemia)	Cuvette	1200	8	99	n/s	c, e	[4]
	Sp2 (myeloma)	μSlide	2∼3k	1	20	n/a	a, g	[44]
Other Cells	Cardiac cell (Frog)	Single cell	0.4 V[A]	1	10 ms	n/a	d	[6]
	Cardiac cell (Pig)	Single cell	3.6[B]	2	10 ms	0.2	b	[7]
	RBC (mouse)	μChannel	1100∼1200	n/a	100∼300 ms	n/a	f	[5]
	WBC (mouse)	μChannel	400∼500	n/a	100∼300 ms	n/a	a	[5]

[*] n/a- not applicable, n/s- not specified.
[#] a- Membrane integrity dye (PI, Hoechst, Trypan blue, etc.), b- Voltage sensitive dye (di-8-ANEPPS, etc.), c- NAD(P)H dependent cellular oxidoreductase enzymes (MTT, XTT, CCK, etc.), d- Electrical properties (current, voltage), e- ATP assay, f- RBC ghosts, g- Volumetric assay.
^ unless otherwise noted.
A-Micro-pipette tip suction, B-chamber field.

environmental conditions that affect the cell metabolic activity can alter the cell viability results as well.

Finally, ATP is a molecule found in and produced by living cells that can be measured and used as a viability assay. Specifically, ATP levels can be quantified by measuring the light emitted through its reaction with luciferase reagents using a luminometer. The amount of light produced is directly proportional to the amount of living cells present in the sample. ATP assay can suffer from similar limitations of the NAD(P)H-based assays in that it is unable to differentiate metabolically mute cells from dead ones and can also vary with the environmental conditions.

D. IRE Parameters and Outcomes

This section is an attempt to tabulate and compare the IRE parameters between the *in vitro* studies that have been published using the above assays to date. Due to the wide variations of experimental configurations and evaluation methods, the choice of IRE parameters varies greatly among studies reviewed in Table I. The applied electric field can range from hundreds to thousands of V/cm. The pulse number can range from 1 to more than 3800, and pulse duration can range from under 100 μs to 300 ms. Unfortunately, most studies did not report pulsing frequency, which is also an influential parameter in electroporation [58], [95]. In terms of injury assessment, more than half the studies have chosen membrane dye or NAD(P)H-based assay (or both) as their viability assay. Some studies have adopted the viability assay that is more specific to their choice of cell line (e.g., the RBC ghost assay).

One of the first systematic studies of parameters needed for IRE of cancer cells was performed *in vitro* by Rubinsky's group using cell suspensions in a cuvette [16]. In this study, the researchers tested IRE electric field strengths in the range of 125 V/cm to 2000 V/cm, and pulse numbers from 1 to 3840 (see Fig. 5). The pulse duration was kept constant in this study at 100 μs. A total of 90 pulses at 250 V/cm for 100 μs separated by 100 ms were found to completely destroy prostate cancer cells without inducing thermal damage. Counter to most studies they found that lower electrical fields can be more effective than higher fields for IRE. However, they did not provide data on the influence of each individual parameter (i.e., varying electric field, pulse number, and pulse duration independently while keeping the other two constant). Nevertheless, this was the beginning of systematic study of IRE parameters for cell destruction.

A more recent overview of electroporation parameters on IRE has been presented by Weaver *et al*. [32]. Here, combinations spanning three orders of magnitude in pulse strength (i.e., electric field) and nine orders of magnitude in pulse duration were discussed. In this review as with the bulk of the literature, higher field strengths (1–10 kV/cm) and longer pulses (μs–ms) were more successful at inducing IRE. Although this destruction appears to be necrotic, even higher field strengths (10–100 kV/cm) and shorter pulses ($<\mu$s) led to apoptosis (an emerging concept called supra electroporation). Finally, lower field strength and short pulses tend to lead to survival, which appears to be in conflict with Rubinsky's original paper [16]. This may demonstrate the need for simultaneously varying all three parameters in a single cell type to fully explore biological response to electroporation.

To assess all three IRE parameters independently, our group recently performed an *in vitro* study in a prostate cancer cell line (LNCaP Pro 5) and a cardiac cell line (HL-1) using the cuvette cell suspension setup (see Fig. 6) [96]. We observed that due to the stochastic nature of IRE, even high electric fields cannot guarantee death of the entire cell population if the pulse number or duration is low. For instance in the HL-1 case, the viability first starts to drop below 90% when electrical field exceeded 750 V/cm. This number can be considered as a lower threshold for this cell type. Complete cell death (greater than 90%) can be achieved when the electric field is above 1250 V/cm

Trypan blue test results of PC3 cell viability after nonthermal IRE at range of fields and number of pulses

	No. Alive/No. Dead (% alive)			
	Trial 1	Trial 2	Trial 3	Mean ± SD % Alive
Control	80/0 (100.0)	90/0 (100.0)	50/0 (100.0)	100
IRE:				
2,000 V/cm, 10, 100 μsec pulses	65/25 (72.2)	74/25 (74.7)	33/19 (63.5)	70 ± 6
1,500 V/cm, 17, 100 μsec pulses	53/30 (63.9)	35/50 (41.2)	32/19 (62.7)	56 ± 12
1,000 V/cm, 60, 100 μsec pulses	35/60 (36.8)	23/60 (27.7)	10/45 (18.2)	27 ± 9
750 V/cm, 106, 100 μsec pulses	7/50 (12.3)	7/83 (7.8)	11/60 (15.5)	12 ± 4
500 V/cm, 240, 100 μsec pulses	0/80	0/90	0/50	0.0
250 V/cm, 960, 100 μsec pulses	0/80	0/90	0/50	0.0
125 V/cm, 3,840, 100 μsec pulses	0/80	0/90	0/50	0.0

Flow cytometry results of PC3 cell viability after nonthermal IRE at range of fields and number of pulses

	No. Alive/No. Dead (% alive)			
	Trial 1	Trial 2	Trial 3	Mean % Alive
Control	10/0 (100)	10/0 (100)	10/0 (100)	100
IRE:				
2,000 V/cm, 10, 100 μsec pulses	8/2 (80)	8/2 (80)	8/2 (80)	80
1,500 V/cm, 17, 100 μsec pulses	6/4 (60)	6/4 (60)	6/4 (60)	60
1,000 V/cm, 60, 100 μsec pulses	3/7 (30)	3/7 (30)	3/7 (30)	30
750 V/cm, 106, 100 μsec pulses	1/9 (10)	1/9 (10)	1/9 (10)	10
500 V/cm, 240, 100 μsec pulses	0/10	0/10	0/10	0
250 V/cm, 960, 100 μsec pulses	0/10	0/10	0/10	0
125 V/cm, 3,840, 100 μsec pulses	0/10	0/10	0/10	0

Fig. 5. Test results of PC3 cell viability after nonthermal IRE at range of fields and number of pulses [16]. Reprinted with permission from Elsevier.

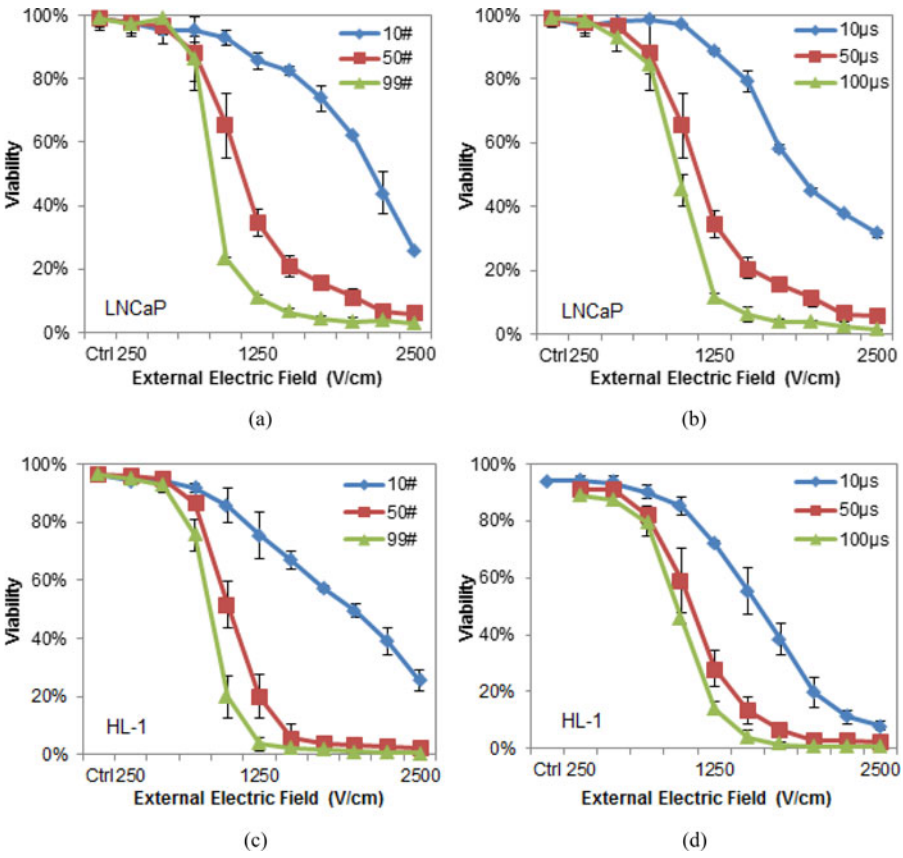

Fig. 6. Test results of cell viabilities after IRE: (a) LNCaP Pro5 viability as a function of changing electric field and pulse number, pulse duration is 50 μs, (b) LNCaP Pro5 viability as a function of changing electric field and pulse duration, pulse number is 50, (c) HL-1 viability as a function of changing electric field and pulse number, pulse duration is 50 μs, and (d) HL-1 viability as a function of changing electric field and pulse duration, pulse number is 50. Injury assessment method for (a) and (b) is CCK-8 cell viability assay, for (c) and (d) is double dye staining assay (Hoescht and PI). Pulse frequency for each case is 10 Hz. Each data point represents the average of $n \geq 3$ measurements ± SD.

given sufficient pulse number or duration. In between 750 and 1250 V/cm, the cells are injured but may not actually die as a result of acute IRE injury. It is worth noting that in our study, when the electric field is lower than 500 V/cm, simply increasing the pulse number or duration does not lead to higher cell injury. This is also contradictory to Rubinsky's study [16], in which complete cell death (100%) can be achieved for electric field as low as 125 V/cm. However, the pulse number range in our study (up to 90) is far less than that in Rubinsky's study (up to 3840). It would be interesting to investigate low electric field (lower than 500 V/cm) induction of complete cell death from IRE given sufficient pulse number, and how this can be related to clinical applications. It is worth noting that pulse repetition frequency and timing (delay between pulses) can also influence the outcome of IRE therapy [58], [95]. The same pulse generator (BTX ECM 830) and pulsing frequency (10 Hz) were used in the above two studies.

In summary, despite some variations, general trends do appear to hold from these studies. For example, the majority of field strengths used in *in vitro* IRE studies fall between 1000–2000 V/cm, which is above the theoretical threshold calculation of 667 V/cm to induce IRE injury as discussed with (1) and in previous work by Weaver and Chizmadzhev [29]. Both pulse number and duration have major impact on the electric field threshold and need to be carefully accounted for during IRE treatment planning. Finally, pulse repetition frequency and timing can also influence the outcome of IRE and should be considered when comparing results from different studies.

IV. Translational Studies of IRE

Since Davalos *et al*. [15] first proposed the use of electroporation as a means of soft tissue destruction, a great number of preclinical tests have been undertaken to support this new modality. Among them, *in vivo* testing on animal organs has generated the most abundant data and useful conclusions so far. The goal of this section is to summarize these experimental findings and categorize them in a manner that is readily available for clinicians and researchers relatively new to the field. A complete summary of these *in vivo* studies can be found in Table II and will be the basis of our discussion in the following sections.

A. Tissue IRE Electrodes

There are four major types of IRE electrodes: plate, needle, clamp, and catheter. Their popularity in usage can be found in Fig. 7(a). The plate electrode design delivers the electric field by placing two parallel plate electrodes across the target tissue. It can provide homogeneous electric field distribution between the plate electrodes in the target area. The electric field is easy to determine and is relatively well constrained between the two plates. However, plate electrodes are much more invasive if they need to be placed inside the body. Their usage can also be limited due to the difficulty of placement and having to maintain the relative parallel position between the two plates. Therefore, they are more often considered when the target tissue is more easily accessible (e.g., during an open surgery). The needle electrodes are the most popular selection reviewed (58% of all cases) for tissue destruction. In this design, the cathode and/or the anode are integrated onto a needle shaped delivery system, which is inserted to the target site. The needle electrodes are relatively less invasive, yet provide easy manipulation for placement. The number of needle electrode(s) can be one, two, or more [see Fig. 7(b)]. However, the electric field generated by needle electrode(s) is not homogeneous and needs to be carefully calculated before treatment using simulation software [15], [117]. Adding electrode number and optimizing the electrode placement can help increase the effective treatment volume, but this can make the treatment more invasive and complicate the procedure [118]. In the clamp electrode design, the cathode and the anode are integrated onto the inner faces of a clamp, which is used to hold the target tissue from the outside. The clamp design can also be invasive and suffers similar limitations as the plate electrode. However, it can provide more secure contact that works better for specific organs, such as arteries and intestines, during open surgery. Finally, in the catheter electrode design, the electrodes are delivered via a catheter inside the tubular organ. Good contact is usually ensured by placing the electrodes on a balloon surface or preshaped nickel titanium (nitinol) wires [115]. It requires specific skill to manipulate and navigate to the target site but can be the least invasive of all the designs.

Several researchers have expressed concerns about the impact of electrode size to the actual treatment volume. For instance, with the needle electrode design, it has been found that the smaller the diameter of the electrode, the higher the voltage needed [98], [117] to create the same treatment volume if all other parameters are the same. This is because the decrease of electric field intensity in the vicinity of the electrodes is steeper at smaller diameters of the electrodes; therefore, the area covered with a given electric field intensity is smaller at smaller diameters of electrodes.

When multiple electrodes are used, the distance between the electrodes [see Fig. 7(c)] and critical organs are critical parameters. For instance, in the heart, Deodhar *et al*. [103] has found that within 1.7 cm from the heart, fatal events occurred with all unsynchronized IRE in a study of 11 pigs with lung and myocardium tissue destructions. ECG synchronized IRE delivery could avoid significant cardiac arrhythmias although minor events still present.

B. IRE Pulse Parameters (Electric Field, Pulse Duration, and Pulse Number)

Although many parameters can influence the outcome of IRE for a given tissue type, the electric field, pulse duration, and pulse number are the most experimentally studied. Importantly, new experimental data suggests that pulse delays can also have dramatic impact on outcome [58], [95]. This suggests the need for additional experimental and theoretical research, as most biomedical technologies eventually need mechanistic support for adoption and full acceptance. It is worth noting that there are discrepancies in the way that the electric field is presented in the literature (i.e., field V/cm versus potential V). We represent what we can glean from these studies in Table II. It can be seen that the majority (89%) of researchers used an electric

TABLE II
SUMMARY OF *In Vivo* IRE STUDIES

Model			Electrode Design			Pulse Parameters			Injury Evaluation	Outcomes / Comments	Ref.
			Type*	Number/ Dist. (mm)	Electric Field (V/cm) or Voltage (V)	Number	Duration (μs)^	Freq. (Hz)^			
Normal Tissue	*Liver*	Rat	P	2/4	1000	1	20 ms	n/a	H	Threshold: 300–500 V/cm Lesion size: 48.6–59.6 mm^2	[20]
									V	Vascular block: transient 15∼20mins	
		Rat	P	2/5	1500	8	100	10	H	Lesion: qualitative	[64]
									E	σ increase: 43+-1%	
		Rat	N	2/5 or 2/10	500 or 1000 V	8	100	10	MRI	Lesion: hyperintense	[97]
									H	Lesion: qualitative	
		Rabbit	N	2/8	860–1360 V	8	100	1	H	Threshold: 637 $\pm$ 43 V/cm	[98]
		Porcine	N	4/15 or 2/25	2500 V	8	100	10	H	Threshold: 600 V/cm.	[23]
									US	Lesions: hypointense during, then hyperintense 24 h after IRE	
		Porcine	P	various	1000	99	100	0.25–4	H	Threshold: 423 $\pm$ 147 V/cm.	[99]
			N	2/5	1500				D	>50% decellularized	
		Rabbit and Porcine	N	1	2500 V	90	100	n/s	H, US, and TTC	Lesion: qualitative	[100]
									US	Pores sizes from 80–490 nm	
	Brain	Rat	N	2/1	50–400 V	90–180	200	250k or 500k	H, MRI	Lesion: qualitative	[101]
									V	Hi-Frequency reduces muscle contraction	
		Dog	N	2/5	500 or 1000 V	90	50	4	MRI, US	Threshold 495∼510 V/cm	[22]
										Lesion size: 0.25∼0.6 cm^3	
									MRI	Lesion: hyperintense	
		Dog	N	2/5	500–1500 V	80	50	0.5, 1, or 4	H, CT	Lesion: qualitative	[102]
									MRI	Lesion size: 0.131 (T1) and 0.12 cm^2 (T2) immediately after IRE, hyperintense for both	
		Dog	N	1 or 2/5–10	500–2000 V	90	50	4	H	Lesion: qualitative	
									MRI	Lesion size: 0.259 cm^2 (500 V), 0.599 cm^2 (1000), 1.665 cm^2 (1500 V). Lesion is hypo-intense under T1-MRI and hyper-intense under T2-MRI.	[25]
	Lung	Porcine	N	2/9 or 2/15	1500 or 2500 V	90	70	4 or ECG synchronized	H, CT	Threshold 500 V/cm. Lesion size:776.4 cm^3.	[103]
									ECG	Distance for IRE to cause heart damage: 1.7 cm.	
	Kidney	Porcine	N	2/9–15	1700–2500 V	90	70	4	H, CT	CT imaging hypodense.	[26]
		Porcine	N	1 or 2/15	2700V (single) or 2700 V (paired)	90	70 or 100	n/s	H	Lesion size: 0.38–2 cm^3 (paired), 0.68–5.6 cm^3 (single). Sizes decrease over time.	[27]
		Porcine	N	1	2700 V	90	70 ms	1.5	A	No acute vascular damage by IRE from real-time DSA monitoring.	[104]
	Prostate	Dog	N	1, 2, or 4/ 10–15	1000–2000 V	1–8 (single) 80 (paired)	100	5–10	H	Voltages lower than 1.5 kV produced little to no contraction in anesthetized animals and paralyzed animals.	[24]
	Intestine	Rat	P	2/1	200 V	50	70	4	H	Signs of recovery showed three-day post-surgery by developing and epithelial layer.	[94]

TABLE II
SUMMARY OF *In Vivo* IRE STUDIES

Model			Electrode Design			Pulse Parameters					
			Type*	Number/ Dist. (mm)	Electric Field (V/cm) or Voltage (V)	Number	Duration (μs)^	Freq. (Hz)^	Injury Evaluation	Outcomes / Comments	Ref.
Implanted Tumor		Mice	P	2/3–5	2000 or 2500	80	100, 800, or 1000	0.03–5k	H, TR	Up to 92% complete tumor regression (three weeks).	[21]
		Mice	P	2/4	2500	64	100	1	H, TR	Immune response not necessary for focal IRE efficacy.	[105]
		Mice	P	2/8	1300	8	100	1	US, TR, FI, PO	Rapid decline in perfusion after IRE.	[13]
		Mice	P	2/15–30	2500	8 or 80	100 or 1000	0.03–10	H, E	Increase of conductivity, σ: 10–180%.	[106]
		Mice	N	1	1300 V	100	100	0.3	H, TR, FI	Threshold 1000 V/cm. Lesion size: 5–8 mm. Five of seven cases led to complete regression.	[107]
		Mice DSFC	N	1	500 V	10–99	10–100	10	H, FI	Threshold: 600—1300 V/cm. Lesion size: ~3.5 mm radius	[108]
		Rat	N	2/10	2500 V	8	100	10	H, MRI, TR	IRE lesion is hypointense under T1-MRI and hyperintense under T2-MRI. 52% decrease in tumor size after 15 days.	[28]
Spontaneous Tumor	*Brain*	Dog	N	2/5	500 and 625 V	40 (500 V), 80 (625 V)	50	ECG synchronized	MRI, TR	74.2% average tumor volume reduction with T1-MRI 48 h after IRE.	[109]
		Dog	N	2/5	625 and 500 V	80	50	~1	MRI, CT	Lesion size: 0.15–0.24 cm^3 for 500 V and 0.24–0.4 cm^3 for 625 V.	[110]
	Soft Tissue	Dog	N	1 or 2/8–15	800–1500 V	80	70 or 100	1.5	H, CT, TR	52% volume reduction with CT eight days after IRE.	[111]
Cardiovascular	*Artery*	Rat	C	/0.3	3800	10	100	10	H, VS	VSMC 80% less 28 days after IRE, with no apparent damage to ECM and structure.	[112]
		Rat	C	n/s	1750 or 2500	10, 45 or 90	100	1 or 10	H, VS	VSMC 89–94% less 28 days after IRE, with no apparent damage to ECM and structure.	[113]
		Rat	C	/0.4	1700	90	100	1–4	H, VS	VSMC complete ablated after seven days.	[114]
		Rat	C	/0.4	1750	90	100	4	H, VS	VSMC almost completely ablated after seven days.	[115]
			Ca	n/a	>1000					Endothelial layer regenerate by seven days after IRE.	
	Heart	Pig	P	n/s	1500–2000 V	8, 16, or 32	total 1 s to 4 s	5	H	Lesion size: 0.4–1.4 cm depth, 3–3.5 cm length, 0.5–1.0 cm width.	[116]

* P- plate, N- needle, C- clamp, Ca- catheter.

^ Unless otherwise noted.

Injury Evaluation

H: Histology. MRI: MRI. U: Ultrasound. EM: Electron microscopy. CT: CT scanning. ECG: ECG monitoring. D: Density score. A: Angiography. E: Electrical properties. TR: Tumor regression. FI: Fluorescent imaging/ bioluminescence. TTC: TTC Staining. PO: Tissue oxygenation. VSMC: Vascular smooth muscle cells count.

field between 1000 and 2500 V/cm for tissue destruction. The pulse durations ranged from 50 to 100 μs in 87% of the studies reviewed [see Fig. 7(d)]. And finally, the pulse number ranged between 10 and 90 for most studies [see Fig. 7(e)]. As was discussed in our *in vitro* section, it requires a certain amount of cumulative pulse time to achieve complete cell death even when above threshold electric field level. This can be achieved by either increasing the pulse duration or the total pulse number. However, there are constraints on increasing pulse duration due to Joule heating (i.e., thermal effects) [119], and procedure time is lengthened by increasing pulse number.

C. Injury Evaluation

The injury evaluation in tissue is more complex than *in vitro* or cell cases. For instance, the injury can be monitored in real time intraoperatively or after a procedure in an acute or chronic manner. The injury can also be evaluated on live animals, or

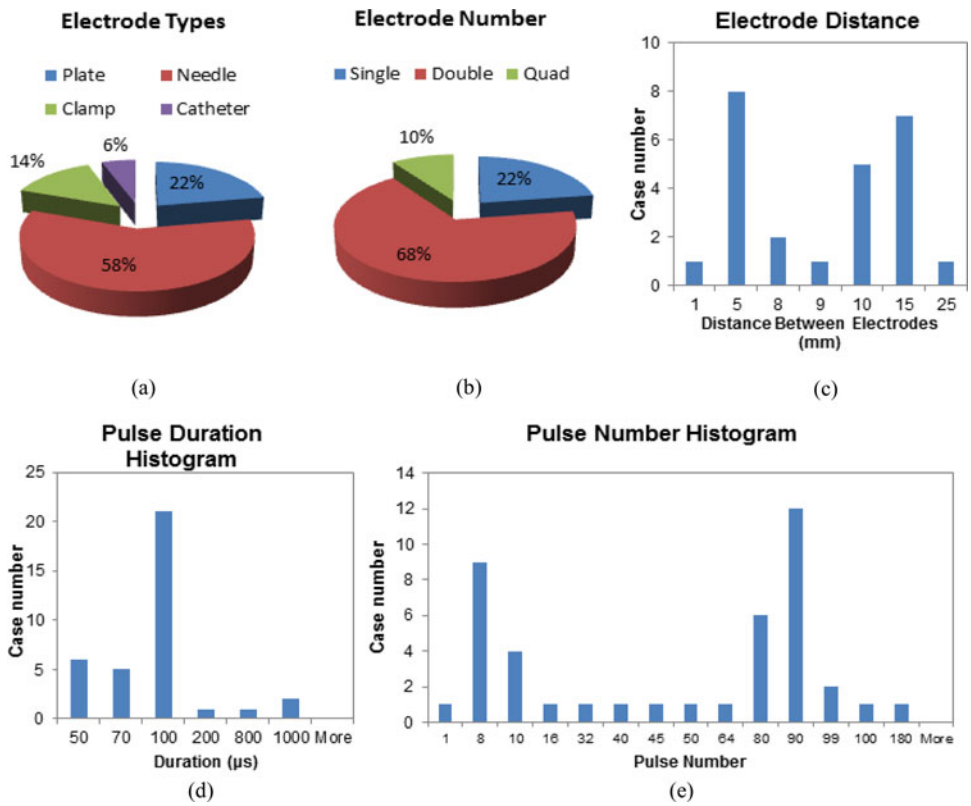

Fig. 7. Distribution of IRE electrode design and parameter choices from Table II. For each electrode type, please refer to [20], [106] (plate), [23] (needle), and [115] (clamp and catheter) for photos and configurations.

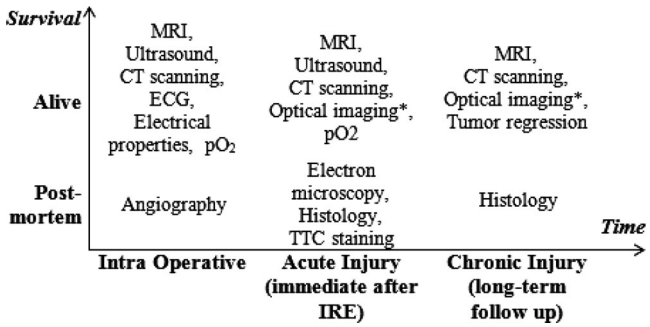

Fig. 8. Choices of injury evaluation method for *in vivo* IRE studies from Table II. *Optical imaging methods are limited by penetration depth, and therefore are used predominantly in intravital chamber systems [58], [108], [120].

postmortem. The injury evaluation methods used are summarized in Fig. 8.

MRI, Ultrasound, and CT scanning are all direct noninvasive imaging methods for live animals. They can be performed any time before, during, or after the procedure. A good review on imaging methods for IRE tumor treatments is given in [121]. Using these modalities, the IRE lesion has been shown to be hypointense under T1-MRI or hyperintense under T2-MRI by Guo *et al.* [28] or hyperintense for both TI and T2 MRI in [22], [102]. In the case of ultrasound, lesions were shown to be hypointense during, and hyperintense 24 h after IRE [23], [122], [123]. Finally, for CT imaging, both intraoperative and follow up scans found hypodense nonenhancing lesion [26]. Not all studies have detailed imaging methods and results, and some studies appear contradictory suggesting an opportunity for further work.

Histological assessment of (usually H&E) stained samples is the most used evaluation method for IRE therapy postmortem [23], [64], [97], [98]. The lesion volume measured from the histology sample can vary greatly depending on the time after IRE treatment, as was described as injury development *in vivo* [23], [112]. In general, follow-up to a minimum of three days is necessary to evaluate the injury development unless only acute injury is of interest.

TTC (Triphenyl tetrazolium chloride) staining is similar to the NAD(P)H-based assay for *in vitro* assessment and is used to differentiate metabolically active and inactive tissues. Compared to histology staining, TTC is faster and less expensive. However, the TTC stained samples cannot be stored and used at a later time like the histology samples. Both the start and incubation timing can affect the viability results. Therefore, careful study is necessary to establish the TTC timing for a specific tissue of interest [124], [125].

Optical methods can use fluorescent dyes in intravitally imaged tissues (i.e., dorsal skin fold) to examine the perfusion defects after IRE treatment. Like the histological assessment, perfusion defects can change as the injury develops in tissue. However, since the same animal can be imaged repeatedly over time, intravital approaches typically require less animals and

money to study the injury compared to histology [58], [108], [126] or tumor growth delay.

Tumor regression or growth delay is another method to determine the treatment efficacy of IRE. Although tumor regression results have been reported in some studies [107], [109], [122], large-scale randomized animal studies are still not available on IRE therapy at this time.

Since IRE is still more often used in combination with chemotherapy or other enhancement reagents, the influence of chemo drug (bleomycin or other cytotoxic agents) or adjuvants on the viability results needs to be carefully accounted for. Specifically, it is important not to confuse the combinatorial IRE therapy outcomes with independent IRE monotherapy, as the results of the two are not directly comparable.

D. Outcomes and Thresholds

The IRE thresholds are mainly determined by overlapping the modeled electric field distribution with the lesion volume measured from viability studies. Most *in vivo* studies have found the threshold to be 500–1000 V/cm (see Table II). It is important to note that the field thresholds reported *in vivo* are highly dependent on how the researchers calculated the field distribution in the tissue. In addition, care should be taken when comparing *in vivo* to *in vitro* due to a number of factors, in particular difference in cell shape. Nevertheless, *in vitro* studies can help glean insight into the roles of secondary parameters such as pulse duration and repetition rate. The lesion size determined by these studies varies greatly due to different viability assays and timing of assessment (intraoperative, post treatment, etc.) and different tissue/animal subject. In general, the IRE treatment volume is relatively small in our surveyed studies [25], [28], [63], [116]. Although one could consider the use of high voltages in the living body to be a safety concern, it is important to realize that the energy delivered is extremely low due to the short duration of the pulses. IRE usages were shown to be safe during tissue destruction in the studies surveyed here. Specifically, all animals treated with IRE survived after the treatment and only few cases have reported side effects associated with electrical shocking such as temporal muscle contraction and arrhythmia [23], [103]. More recent studies have adopted ECG synchronized IRE combined with general anesthesia to address the above side effects.

V. Clinical Studies

Electroporation has been used clinically for more than 15 years in combination with chemotherapy, and is on the rise as a monotherapy over the last five years. Internationally, there are a number of ongoing clinical trials of IRE therapy [118], [127]–[133]. In 2010, Pech *et al*. [128] (Germany) reported the first in-man clinical study with IRE treatment on kidney ($n = 6$). The study was for safety verification only. The tumors were surgically resected 5 min after IRE, and no treatment protocol was recorded in that paper. In 2011, Thomson *et al*. [129] (Australia) published a larger scale study of various organs. They investigated ECG synchronized IRE in 38 humans with advanced malignancy of liver ($n = 25$), kidney ($n = 7$), and lung ($n = 3$), a total of 69 separate tumors (average $= 46$ cm^3). Tumor destruction verified by CT was achieved in 66% (46/69) tumors. Complications found in this study include cardiac arrhythmia, temporary plexus injury, partial ureteric obstruction, and short-term post-procedure pain. In 2013, Robert *et al.* [132] (Australia) reported another IRE study on 11 patients with 18 unresectable hepatocellular carcinoma that were not suitable for RF treatment. The mean follow-up period was 18 months. Thirteen of the 18 (72%) lesions were completely destroyed. The translated to a 93% success rate for lesions ≤ 3 cm (13/14). The local recurrence-free period was 18 ± 4 months and the distance recurrence-free period was 14 ± 6 months. No serious complications were observed in this study, although minor issues such as transient urinary retention, transient local post-procedure pain, and lesions lying adjacent to important structures or organs. In 2014, Neal *et al*. [134] (Australia) reported two cases of IRE treatment of prostate cancer 3–4 weeks before surgical resection to evaluate safety and characterize the relevant properties to improve treatment planning and outcome predictions. IRE has also been investigated for locally advanced pancreatic cancer in a series of studies by Martin *et al*. [133], [135] and found to be safe and effective at local management of the disease.

A further list of clinical trials that are recruiting patients and registered in the U.S. can be found in Table III. From this table, we can see that the number and scale of clinical studies on IRE have greatly increased since 2013 (see Fig. 9). A systematic review of the safety and efficacy of IRE therapy in clinical setting can be found in [136].

VI. Limitations and Challenges of IRE

Despite the advantage and progress discussed above, IRE is still not the preferred choice of treatment for most diseases. IRE is usually considered only when other therapies are not applicable or fail to show an improvement. This lack of acceptance of IRE within the medical community is due in part to the status of development of the technology, and to several issues with the outcomes of IRE. Specifically, IRE has shown an inability to destroy large volumes of tissues without repetition or repositioning the electrodes. This is an important limitation that remains to be fully addressed. For instance, the common lesion sizes reviewed in Table III using one pair of electrodes without repositioning the electrodes are <1 cm^3 [25], [28], [63], [116]. This is because larger electric fields (i.e., ≥ 2500 V/cm) needed to create larger lesions may increase the damage to adjacent nerves and the cardiovascular system [103], [137]. One approach to circumvent these high fields while treating larger lesions is to use multiple electrodes or repeat treatment with repositioned electrodes. Theoretically, with well-planned electrode layouts, a larger and customized lesion could be achieved to completely destroy a target tumor. However, the addition of multiple electrodes increases the complexity and difficulty of the procedure and makes the treatment more invasive.

A further limitation of IRE treatment is the resulting heterogeneity of injury within the target treatment zone. For instance, some studies [28], [108] now show that incomplete treatment (live tumor patches in a target treated zone) have been found after IRE, leading to concerns such as recurrence. If unresolved, this represents a threat to the translation of IRE. Importantly, local

TABLE III
CLINICAL TRIALS OF INDEPENDENT IRE STUDIES REGISTERED ON CLINICTRIALS.GOV

NCT Study #	Start/Finish Time	Patient #	Country	Target	Endpoint (Phase #)
NCT01078415	Feb 2010, Oct 2011	25	France, Germany, Italy, Spain	Carcinoma, Hepatocellular	S/E*
NCT01442324	Feb 2011, Sep 2012	5	Italy	Metastatic Liver Cancer;Cholangio-carcinoma;Neop-lasm Metastasis	S/E
NCT01369420	May 2011, Dec 2011	10	Italy	Pancreatic Adenocarcinoma	S (2)
NCT02010801	Apr 2012, Dec 2013	20	Taiwan	Malignant Liver Tumors	n/a
NCT01799044	Nov 2012, Sep 2013	10	Netherlands	Colorectal Liver Metastases; Metastatic Liver Disease	S/E (1)
NCT01790451	Aug 2013, Mar 2014	16	Netherlands	Prostate Cancer	S/E (1)
NCT01939665	Sep 2013, Sep 2014	10	Netherlands	Pancreatic Cancer	S/E (1,2)
NCT01726894	Oct 2013, April 2015	20	U.K.	Prostate Cancer	n/a
NCT01967407	Oct 2013, Dec 2015	20	Germany	Kidney Tumor; Renal Cell Cancer	E (1,2)
NCT01972867	Nov 2013, July 2014	6	U.S.	Prostate Cancer	S
NCT01835977	Jan 2014, Jan 2018	200	Netherlands	Prostate Cancer	S/E (2)

*S-Safety, E-Efficacy.

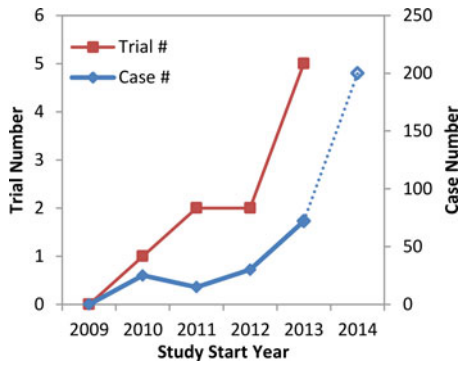

Fig. 9. Numbers of IRE clinical trials that are recruiting patients and registered in the U.S. from Table III.

recurrence after hyperthermia and cryosurgery is significant and reported in the clinical literature [138]–[140]. However, having studied preclinical lesions for IRE, heat, and cryo in an identical animal model, the appearance of live tumor patches within the treated tumor volume (rather than at the boundary) appears at this stage to be unique for electroporation [108], [141]. It is possible that the live cell patches are a result of local electrical property heterogeneity within the tumor tissue, thereby lowering the effective electric field in the target region [142]. Thus, a key challenge to IRE cancer therapy is how to ensure the electric field distribution over the entire target region is above the IRE threshold. This can be achieved through pretreatment planning and monitoring electric field distribution [90], [91], or by enhancements that either alter the field impact and/or reduce the IRE threshold in the tissue [58], [74].

VII. POTENTIAL ENHANCEMENT APPROACHES

A. Cytotoxic Agents

In recognition of the smaller volume or potential for heterogeneous response within the tissue, several groups have already championed a combinatorial approach as mentioned earlier in the review entitled: "electrochemotherapy." This method uses electroporation to allow chemotherapeutics such as bleomycin, which are normally not taken up by cells, to more easily internalize and destroy cells and is reviewed in more detail elsewhere [12], [13]. A similar method proposed by Frandsen *et al.* [68] uses direct intratumoral calcium injection followed by electroporation, leading to lethal intracellular calcium events. While promising, cytotoxic drug or molecules are still limited by the dose and side effects, thus further methods remain of interest to research and clinical groups.

B. Use of High-Frequency IRE

High-Frequency IRE (H-FIRE) is another promising enhancement approach for IRE therapy. Unlike conventional IRE, H-FIRE protocols involve the use of microsecond bursts of bipolar pulses on the order of 500 ns to 5 μs, delivered at a pulse repetition rate of 1 Hz [101], [143]. The benefit of H-FIRE is that it provides the ability to administer IRE therapy without the use of neuroblocking agents to mitigate muscle contractions during the procedure [101]. In addition, high-frequency fields have the potential to overcome impedance barriers posed by low-conductivity tissues, which could provide more predictable lesion volumes. For instance, H-FIRE may mitigate the effects of patient-to-patient tissue variability, conductivity changes due to electroporation, and tissue heterogeneities [143]. While H-FIRE is a relatively unexplored area of research, it may prove interesting if a positive relationship between H-FIRE parameters and larger treatment volumes can be established [32].

C. Membrane Modifications

Another class of studies focuses on enhancing the destructive efficacy of IRE itself without relying on chemotherapeutic drugs or cytotoxic agents to enter and kill the cancer cells. Specifically, approaches that directly modify membrane properties (i.e., line tension and surface tension) by surfactants, impeding the resealing process (big molecules, channel holders, etc.), and fine tuning the pulse timing have all been tried and shown effective in enhancing the IRE destructive potential, as summarized in Table IV.

For instance, one study on IRE enhancement with DMSO has shown that over 60% increase in cell destruction *in vitro* and greater than 136% increase in treatment volume *in vivo* can be achieved by adding 5% volume percentage of DMSO

TABLE IV
MEMBRANE TARGETED ENHANCEMENTS FOR IRE

	Model	Adjuvant	Dose	Timing	Injury Eva.	Indications	Ref.
Surfactant addition	Prostate cancer cells	DMSO	1–15% v/v	1 min before IRE	PI and Hoechst	$>$75% increase in cell destruction	[145]
	Mice DSFC tumor	DMSO	5% v/v	6 min before IRE	Histology, intravital imaging	$>$136% increase in injury volume	[58]
	Lipid bilayer	$C_{12}E_8$	0.1 μM			Lower threshold voltage	[74], [144]
	Pig skin	SDS(sodium dodecyl sulfate)					[146], [147]
Channel effect	Lipid bilayer	Gramicidin D	conc. $>$1:500			Increase threshold voltage	[148]
	Lipid bilayer	a-hemolysin					[149]
Pore holder	Pig skin	Heparin					[150]
	Pig skin	Sodium thiosulfate					[151]
Pulse timing	Prostate cancer cells	n/a	n/a	three trains, 10 s to 2 min delays	PI and Hoechst	$>$67% increase in cell destruction	[145]
	Mice DSFC tumor	n/a	n/a	three trains, 30 s delays	Histology, intravital imaging	$>$101% increase in injury volume	[58]

to the cell suspension or perfused into the tissue [58]. Another study on a lipid bilayer model has shown that as low as 0.1 μM of $C_{12}E_8$ can lower the IRE transmembrane voltage threshold from 450 to 333 mV [74]. The enhancement effect of $C_{12}E_8$ has also been studied *in vitro* [144]. Moreover, studies have shown that simply varying the timing of the pulses without changing the total pulse number or electric field can increase the cell destruction by 67% *in vitro* [145] and tissue destruction volume by 101% in *vivo* [58], respectively. Because the pulse timing approach does not introduce any foreign molecules into the body, it enhances the efficacy of IRE with no additional cost beyond fractionally longer treatment times (minutes). Further, it can be combined with existing IRE protocols (with or without other enhancements).

The number and variety of studies on IRE enhancement is still limited at this time. However, initial results are promising, suggesting that enhancement can increase the treated volume thereby potentially addressing one of the major hurdles to effective clinical translation.

VIII. CONCLUSION

Although IRE was only introduced less than a decade ago, numerous preclinical and clinical studies have been conducted to characterize its destructive potential for different cancer types. Many encouraging results have been reported and unique benefits have been observed in IRE compared to other focal therapies. However, to help establish IRE as a reliable cancer treatment modality in the clinic, further understanding of injury mechanisms, different cell and tissue response, and feedback from imaging approaches are still needed. Future opportunities also exist in establishing well-defined treatment planning protocols, improving the treatment delivery methods, and optimizing treatment outcomes with enhancement approaches.

ACKNOWLEDGMENT

The authors would like to thank G. Long and P. Shires for insightful discussions and encouragement in compiling this review and performing enhancement studies.

REFERENCES

[1] J. C. Weaver, "Electroporation of cells and tissues," *IEEE Trans. Plasma Sci.*,, vol. 28, no. 1, pp. 24–33, Feb. 2000.
[2] A. Ivorra and B. Rubinsky, *Irreversible Electroporation*. Berlin, Germany: Springer, 2010, pp. 1–21.
[3] R. Stampfli, "Reversible electrical breakdown of the excitable membrane of a Ranvier node," *Acad. Bras. Cienc.*, vol. 30, pp. 57–63, 1958.
[4] A. J. H. Sale and W. A. Hamilton, "Effects of high electric fields on microorganisms: I. Killing of bacteria and yeasts," *Biochim. Biophys. Acta BBA Gen. Subj.*, vol. 148, no. 3, pp. 781–788, Dec. 1967.
[5] M. J. Jaroszeski *et al.*, "In vivo gene delivery by electroporation," *Adv. Drug Del. Rev.*, vol. 35, no. 1, pp. 131–137, Jan. 1999.
[6] L. M. Mir, "Therapeutic perspectives of in vivo cell electropermeabilization," *Bioelectrochemistry*, vol. 53, no. 1, pp. 1–10, Jan. 2001.
[7] J. Gehl, "Electroporation: Theory and methods, perspectives for drug delivery, gene therapy and research," *Acta Physiol. Scand.*, vol. 177, no. 4, pp. 437–447, Apr. 2003.
[8] M. Okino and H. Mohri, "Effects of a high-voltage electrical impulse and an anticancer drug on in vivo growing tumors," *Jpn. J. Cancer Res.*, vol. 78, no. 12, pp. 1319–1321, 1987.
[9] D. Miklavčič *et al.*, "Electrochemotherapy: From the drawing board into medical practice," *Biomed. Eng. OnLine*, vol. 13, no. 1, p. 29, Mar. 2014.
[10] R. Cadossi *et al.*, "Locally enhanced chemotherapy by electroporation: Clinical experiences and perspective of use of electrochemotherapy," *Future Oncol.*, vol. 10, no. 5, pp. 877–890, Apr. 2014.
[11] G. A. Hofmann *et al.*, "Electroporation therapy: A new approach for the treatment of head and neck cancer," *IEEE Trans. Biomed. Eng.*, vol. 46, no. 6, pp. 752–759, Jun. 1999.
[12] A. Gothelf *et al.*, "Electrochemotherapy: Results of cancer treatment using enhanced delivery of bleomycin by electroporation," *Cancer Treat. Rev.*, vol. 29, no. 5, pp. 371–387, Oct. 2003.
[13] G. Sersa *et al.*, "Vascular disrupting action of electroporation and electrochemotherapy with bleomycin in murine sarcoma," *Brit. J. Cancer*, vol. 98, no. 2, pp. 388–398, Jan. 2008.
[14] L. M. Mira *et al.*, "Standard operating procedures of the electrochemotherapy: Instructions for the use of bleomycin or cisplatin

administered either systemically or locally and electric pulses delivered by the Cliniporator TM by means of invasive or non-invasive electrodes," *CR Acad. Sci. Paris*, vol. 313, pp. 613–618, 2006.
[15] R. V. Davalos *et al.*, "Tissue ablation with irreversible electroporation," *Ann. Biomed. Eng.*, vol. 33, no. 2, pp. 223–231, Feb. 2005.
[16] J. Rubinsky *et al.*, "Optimal parameters for the destruction of prostate cancer using irreversible electroporation," *J. Urol.*, vol. 180, no. 6, pp. 2668–2674, Dec. 2008.
[17] N. Bao *et al.*, "Microfluidic electroporation of tumor and blood cells: Observation of nucleus expansion and implications on selective analysis and purging of circulating tumor cells," *Integr. Biol. Quantum Biosci. Nano Macro*, vol. 2, no. 2–3, pp. 113–120, Mar. 2010.
[18] L. Miller *et al.*, "Cancer cells ablation with irreversible electroporation," *Technol. Cancer Res. Treat.*, vol. 4, no. 6, pp. 699–705, Dec. 2005.
[19] H. Shafiee *et al.*, "A preliminary study to delineate irreversible electroporation from thermal damage using the Arrhenius equation," *J. Biomech. Eng.*, vol. 131, no. 7, pp. 074–509, Jul. 2009.
[20] J. F. Edd *et al.*, "In vivo results of a new focal tissue ablation technique: Irreversible electroporation," *IEEE Trans. Biomed. Eng.*, vol. 53, no. 7, pp. 1409–1415, Jul. 2006.
[21] B. Al-Sakere *et al.*, "Tumor ablation with irreversible electroporation," *PLoS ONE*, vol. 2, no. 11, p. e1135, Nov. 2007.
[22] P. A. Garcia *et al.*, "Intracranial nonthermal irreversible electroporation: In vivo analysis," *J. Membr. Biol.*, vol. 236, no. 1, pp. 127–136, Jul. 2010.
[23] B. Rubinsky *et al.*, "Irreversible electroporation: A new ablation modality-clinical implications," *Technol. Cancer Res. Treat.*, vol. 6, no. 1, pp. 37–48, Feb. 2007.
[24] G. Onik *et al.*, "Irreversible electroporation: Implications for prostate ablation," *Technol. Cancer Res. Treat.*, vol. 6, no. 4, pp. 295–300, Aug. 2007.
[25] T. L. Ellis *et al.*, "Nonthermal irreversible electroporation for intracranial surgical applications," *J. Neurosurg.*, vol. 114, no. 3, pp. 681–688, Mar. 2011.
[26] A. Deodhar *et al.*, "Renal tissue ablation with irreversible electroporation: Preliminary results in a porcine model," *Urology*, vol. 77, no. 3, pp. 754–760, Mar. 2011.
[27] C. R. Tracy *et al.*, "Irreversible electroporation (IRE): A novel method for renal tissue ablation," *BJU Int.*, vol. 107, no. 12, pp. 1982–1987, Jun. 2011.
[28] Y. Guo *et al.*, "Irreversible electroporation therapy in the liver: Longitudinal efficacy studies in a rat model of hepatocellular carcinoma," *Cancer Res.*, vol. 70, no. 4, pp. 1555–1563, Feb. 2010.
[29] J. C. Weaver and Y. A. Chizmadzhev, "Theory of electroporation: A review," *Bioelectrochem. Bioenerg.*, vol. 41, no. 2, pp. 135–160, 1996.
[30] R. C. Lee *et al.*, "Transient and stable ionic permeabilization of isolated skeletal muscle cells after electrical shock," *J. Burn Care Res.*, vol. 14, no. 5, pp. 528–540, 1993.
[31] A. Golberg and M. L. Yarmush, "Nonthermal irreversible electroporation: Fundamentals, applications, and challenges," *IEEE Trans. Biomed. Eng.*, vol. 60, no. 3, pp. 707–714, Mar. 2013.
[32] J. C. Weaver *et al.*, "A brief overview of electroporation pulse strength-duration space: A region where additional intracellular effects are expected," *Bioelectrochemistry*, vol. 87, pp. 236–243, Oct. 2012.
[33] C. Chen *et al.*, "Membrane electroporation theories: A review," *Med. Biol. Eng. Comput.*, vol. 44, nos. 1/2, pp. 5–14, Mar. 2006.
[34] N. Jourabchi *et al.*, "Irreversible electroporation (NanoKnife) in cancer treatment," *Gastrointest. Interv.*, vol. 3, no. 1, pp. 8–18, Jun. 2014.
[35] M. L. Yarmush *et al.*, "Electroporation-based technologies for medicine: Principles, applications, and challenges," *Annu. Rev. Biomed. Eng.*, vol. 16, pp. 295–320, Jul. 2014.
[36] R. C. Lee *et al.*, "Biophysical injury mechanisms in electrical shock trauma," *Annu. Rev. Biomed. Eng.*, vol. 2, no. 1, pp. 477–509, 2000.
[37] A. Ben-Or and B. Rubinsky, *Irreversible Electroporation*. Berlin, Germany: Springer, 2010, pp. 63–83.
[38] T. Kotnik *et al.*, "Cell membrane electroporation—Part 1: The phenomenon," *IEEE Electr. Insul. Mag.*, vol. 28, no. 5, pp. 14–23, Oct. 2012.
[39] M. Pavlin *et al.*, "Chapter seven electroporation of planar lipid bilayers and membranes," in *Advances in Planar Lipid Bilayers and Liposomes*, vol. 6, A. Leitmannova Liu, Ed. San Francisco, CA, USA: Academic, 2008, pp. 165–226.
[40] E. Neumann and K. Rosenheck, "Permeability changes induced by electric impulses in vesicular membranes," *J. Membr. Biol.*, vol. 10, no. 1, pp. 279–290, 1972.
[41] I. G. Abiror *et al.*, "246-electric breakdown of bilayer lipid membranes I. The main experimental facts and their qualitative discussion," *Bioelectrochem. Bioenerg.*, vol. 6, no. 1, pp. 37–52, Mar. 1979.
[42] V. F. Pastushenko *et al.*, "247-electric breakdown of bilayer lipid membranes II. Calculation of the membrane lifetime in the steady-state diffusion approximation," *Bioelectrochem. Bioenerg.*, vol. 6, no. 1, pp. 53–62, Mar. 1979.
[43] Y. Chizmadzhev *et al.*, "248-electric breakdown of bilayer lipid membranes III. Analysis of possible mechanisms of defect origination," *Bioelectrochem. Bioenerg.*, vol. 6, no. 1, pp. 63–70, Mar. 1979.
[44] V. F. Pastushenko *et al.*, "249-electric breakdown of bilayer lipid membranes IV. Consideration of the kinetic stage in the case of the single-defect membrane," *Bioelectrochem. Bioenerg.*, vol. 6, no. 1, pp. 71–79, Mar. 1979.
[45] V. Arakelyan *et al.*, "250-electric breakdown of bilayer lipid membranes V. Consideration of the kinetic stage in the case of the membrane containing an arbitrary number of defects," *Bioelectrochem. Bioenerg.*, vol. 6, no. 1, pp. 81–87, Mar. 1979.
[46] V. F. Pastushenko *et al.*, "251-electric breakdown of bilayer lipid membranes VI. A stochastic theory taking into account the processes of defect formation and death: Membrane lifetime distribution function," *Bioelectrochem. Bioenerg.*, vol. 6, no. 1, pp. 89–95, Mar. 1979.
[47] R. Susil *et al.*, "Electric field-induced transmembrane potential depends on cell density and organization," *Electromagn. Biol. Med.*, vol. 17, no. 3, pp. 391–399, 1998.
[48] W. Krassowska and P. D. Filev, "Modeling electroporation in a single cell," *Biophys. J.*, vol. 92, no. 2, pp. 404–417, Jan. 2007.
[49] G. Pucihar *et al.*, "A time-dependent numerical model of transmembrane voltage inducement and electroporation of irregularly shaped cells," *IEEE Trans. Biomed. Eng.*, vol. 56, no. 5, pp. 1491–1501, May 2009.
[50] K. A. DeBruin and W. Krassowska, "Modeling electroporation in a single cell. I. Effects of field strength and rest potential," *Biophys. J.*, vol. 77, no. 3, pp. 1213–1224, 1999.
[51] K. Kinosita Jr *et al.*, "Electroporation of cell membrane visualized under a pulsed-laser fluorescence microscope," *Biophys. J.*, vol. 53, no. 6, pp. 1015–1019, Jun. 1988.
[52] M. Hibino *et al.*, "Membrane conductance of an electroporated cell analyzed by submicrosecond imaging of transmembrane potential," *Biophys. J.*, vol. 59, no. 1, pp. 209–220, Jan. 1991.
[53] M. Hibino *et al.*, "Time courses of cell electroporation as revealed by submicrosecond imaging of transmembrane potential," *Biophys. J.*, vol. 64, no. 6, pp. 1789–1800, Jun. 1993.
[54] J. M. Crowley, "Electrical breakdown of bimolecular lipid membranes as an electromechanical instability," *Biophys. J.*, vol. 13, no. 7, pp. 711–724, Jul. 1973.
[55] J. D. Litster, "Stability of lipid bilayers and red blood cell membranes," *Phys. Lett. A*, vol. 53, no. 3, pp. 193–194, Jun. 1975.
[56] C. Taupin *et al.*, "Osmotic pressure-induced pores in phospholipid vesicles," *Biochemistry*, vol. 14, no. 21, pp. 4771–4775, Oct. 1975.
[57] J. C. Weaver and R. A. Mintzer, "Decreased bilayer stability due to transmembrane potentials," *Phys. Lett. A*, vol. 86, no. 1, pp. 57–59, Oct. 1981.
[58] C. Jiang *et al.*, "Membrane-targeting approaches for enhanced cancer cell destruction with irreversible electroporation," *Ann. Biomed. Eng.*, vol. 42, no. 1, pp. 193–204, Jan. 2014.
[59] K. T. Powell and J. C. Weaver, "Transient aqueous pores in bilayer membranes: A statistical theory," *Bioelectrochem. Bioenerg.*, vol. 15, no. 2, pp. 211–227, Apr. 1986.
[60] M. Toner and E. G. Cravalho, "Kinetics and likelihood of membrane rupture during electroporation," *Phys. Lett. A*, vol. 143, no. 8, pp. 409–412, Jan. 1990.
[61] D. C. Chang and T. S. Reese, "Changes in membrane structure induced by electroporation as revealed by rapid-freezing electron microscopy," *Biophys. J.*, vol. 58, no. 1, pp. 1–12, Jul. 1990.
[62] R. Benz *et al.*, "Reversible electrical breakdown of lipid bilayer membranes: A charge-pulse relaxation study," *J. Membr. Biol.*, vol. 48, no. 2, pp. 181–204, Jun. 1979.

[63] O. Tovar and L. Tung, "Electroporation and recovery of cardiac cell membrane with rectangular voltage pulses," *Amer. J. Physiol.—Heart Circ. Physiol.*, vol. 263, no. 4, pp. H1128–H1136, Oct. 1992.

[64] A. Ivorra and B. Rubinsky, "In vivo electrical impedance measurements during and after electroporation of rat liver," *Bioelectrochemistry*, vol. 70, no. 2, pp. 287–295, May 2007.

[65] Y. Granot *et al.*, "In vivo imaging of irreversible electroporation by means of electrical impedance tomography," *Phys. Med. Biol.*, vol. 54, no. 16, pp. 4927–4943, Aug. 2009.

[66] R. Shirakashi *et al.*, "Measurement of the permeability and resealing time constant of the electroporated mammalian cell membranes," *Int. J. Heat Mass Transf.*, vol. 47, no. 21, pp. 4517–4524, Oct. 2004.

[67] W. Chen *et al.*, "Supramembrane potential-induced electroconformational changes in sodium channel proteins: A potential mechanism involved in electric injury," *Burns J. Int. Soc. Burn Inj.*, vol. 32, no. 1, pp. 52–59, Feb. 2006.

[68] S. K. Frandsen *et al.*, "Direct therapeutic applications of calcium electroporation to effectively induce tumor necrosis," *Cancer Res.*, vol. 72, no. 6, pp. 1336–1341, Mar. 2012.

[69] H. Schoellnast *et al.*, "The delayed effects of irreversible electroporation ablation on nerves," *Eur. Radiol.*, vol. 23, no. 2, pp. 375–380, Feb. 2013.

[70] R. Heller *et al.*, "Phase I/II trial for the treatment of cutaneous and subcutaneous tumors using electrochemotherapy," *Cancer*, vol. 77, no. 5, pp. 964–971, 1998.

[71] B. Alberts *et al.*, *Essential Cell Biology*. New York, NY, USA: Garland Science, 2013.

[72] G. L. Andreason and G. A. Evans, "Optimization of electroporation for transfection of mammalian cell lines," *Anal. Biochem.*, vol. 180, no. 2, pp. 269–275, Aug. 1989.

[73] S. Y. Ho and G. S. Mittal, "Electroporation of cell membranes: A review," *Crit. Rev. Biotechnol.*, vol. 16, no. 4, pp. 349–362, 1996.

[74] G. C. Troiano *et al.*, "The reduction in electroporation voltages by the addition of a surfactant to planar lipid bilayers," *Biophys. J.*, vol. 75, no. 2, pp. 880–888, Aug. 1998.

[75] P. Kramar *et al.*, "A system for the determination of planar lipid bilayer breakdown voltage and its applications," *IEEE Trans. Nanobiosci.*, vol. 8, no. 2, pp. 132–138, Jun. 2009.

[76] D. K. L. Cheng *et al.*, "Nonuniform responses of transmembrane potential during electric field stimulation of single cardiac cells," *Amer. J. Physiol.-Heart Circ. Physiol.*, vol. 277, no. 1, pp. H351–H362, 1999.

[77] A. V. Somlyo and A. P. Somlyo, "Electromechanical and pharmacomechanical coupling in vascular smooth muscle," *J. Pharmacol. Exp. Ther.*, vol. 159, no. 1, pp. 129–145, Jan. 1968.

[78] J. M. McMahon and D. J. Wells, "Electroporation for gene transfer to skeletal muscles: Current status," *BioDrugs*, vol. 18, no. 3, pp. 155–165, 2004.

[79] A. Lau *et al.*, "A single cell electroporation chip," *Lab. Chip*, vol. 5, no. 1, pp. 38–43, 2005.

[80] J. Olofsson *et al.*, "Single-cell electroporation," *Curr. Opin. Biotechnol.*, vol. 14, no. 1, pp. 29–34, 2003.

[81] J. L. Rae and R. A. Levis, "Single-cell electroporation," *Pflüg. Arch. Eur. J. Physiol.*, vol. 443, no. 4, pp. 664–670, 2002.

[82] M. Wang *et al.*, "Single-cell electroporation," *Anal. Bioanal. Chem.*, vol. 397, no. 8, pp. 3235–3248, 2010.

[83] R. Ziv *et al.*, "Micro-electroporation of mesenchymal stem cells with alternating electrical current pulses," *Biomed. Microdevices*, vol. 11, no. 1, pp. 95–101, Feb. 2009.

[84] A. Kaner *et al.*, "Model of pore formation in a single cell in a flow-through channel with micro-electrodes," *Biomed. Microdevices*, vol. 16, pp. 181–189, Apr. 2014.

[85] T. Y. Tsong, "Electroporation of cell membranes," *Biophys. J.*, vol. 60, no. 2, pp. 297–306, 1991.

[86] K. Kinosita *et al.*, "Events of membrane electroporation visualized on a time scale from microsecond to seconds," in *Guide to Electroporation Electrofusion*. New York, NY, USA: Elsevier, 1992, pp. 29–46.

[87] D. Gross *et al.*, "Optical imaging of cell membrane potential changes induced by applied electric fields," *Biophys. J.*, vol. 50, no. 2, pp. 339–348, 1986.

[88] Y. Rosemberg and R. Korenstein, "Electroporation of the photosynthetic membrane: A study by intrinsic and external optical probes," *Biophys. J.*, vol. 58, no. 4, pp. 823–832, 1990.

[89] E. H. Serpersu *et al.*, "Reversible and irreversible modification of erythrocyte membrane permeability by electric field," *Biochim. Biophys. Acta BBA-Biomembr.*, vol. 812, no. 3, pp. 779–785, 1985.

[90] R. V. Davalos *et al.*, "A feasibility study for electrical impedance tomography as a means to monitor tissue electroporation for molecular medicine," *IEEE Trans. Biomed. Eng.*, vol. 49, no. 4, pp. 400–403, Apr. 2002.

[91] R. V. Davalos *et al.*, "Electrical impedance tomography for imaging tissue electroporation," *IEEE Trans. Biomed. Eng.*, vol. 51, no. 5, pp. 761–767, May 2004.

[92] R. E. Neal *et al.*, "Experimental characterization and numerical modeling of tissue electrical conductivity during pulsed electric fields for irreversible electroporation treatment planning," *IEEE Trans. Biomed. Eng.*, vol. 59, no. 4, pp. 1076–1085, Apr. 2012.

[93] K. Kinosita Jr and T. Y. Tsong, "Voltage-induced conductance in human erythrocyte membranes," *Biochim. Biophys. Acta BBA-Biomembr.*, vol. 554, no. 2, pp. 479–497, 1979.

[94] E. W. Lee *et al.*, "Electron microscopic demonstration and evaluation of irreversible electroporation-induced nanopores on hepatocyte membranes," *J. Vasc. Interv. Radiol.*, vol. 23, no. 1, pp. 107–113, Jan. 2012.

[95] A. Silve *et al.*, "Comparison of the effects of the repetition rate between microsecond and nanosecond pulses: Electropermeabilization-induced electro-desensitization?" *Biochim. Biophys. Acta BBA Gen. Subj.*, vol. 1840, no. 7, pp. 2139–2151, Jul. 2014.

[96] C. Jiang *et al.*, "Comparison of irreversible electroporation, cryo, and thermal ablations on cardiovascular cells," presented at the Design Med. Devices Conf., Minneapolis, MN, USA, 2014.

[97] Y. Guo *et al.*, "Irreversible electroporation in the liver: Contrast-enhanced inversion-recovery MR imaging approaches to differentiate reversibly electroporated penumbra from irreversibly electroporated ablation zones," *Radiology*, vol. 258, no. 2, pp. 461–468, Feb. 2011.

[98] D. Miklavčič *et al.*, "A validated model of in vivo electric field distribution in tissues for electrochemotherapy and for DNA electrotransfer for gene therapy," *Biochim. Biophys. Acta BBA Gen. Subj.*, vol. 1523, no. 1, pp. 73–83, Sep. 2000.

[99] M. B. Sano *et al.*, "Towards the creation of decellularized organ constructs using irreversible electroporation and active mechanical perfusion," *Biomed. Eng. Online*, vol. 9, no. 1, p. 83, 2010.

[100] M. A. Phillips *et al.*, "Irreversible electroporation on the small intestine," *Brit. J. Cancer*, vol. 106, no. 3, pp. 490–495, Jan. 2012.

[101] C. B. Arena *et al.*, "High-frequency irreversible electroporation (H-FIRE) for non-thermal ablation without muscle contraction," *Biomed. Eng. Online*, vol. 10, p. 102, 2011.

[102] P. A. Garcia *et al.*, "A parametric study delineating irreversible electroporation from thermal damage based on a minimally invasive intracranial procedure," *Biomed. Eng. Online*, vol. 10, p. 34, 2011.

[103] A. Deodhar *et al.*, "Irreversible electroporation near the heart: Ventricular arrhythmias can be prevented with ECG synchronization," *Amer. J. Roentgenol.*, vol. 196, no. 3, pp. W330–W335, Mar. 2011.

[104] J. J. Wendler *et al.*, "Angiography in the isolated perfused kidney: Radiological evaluation of vascular protection in tissue ablation by nonthermal irreversible electroporation," *Cardiovasc. Intervent. Radiol.*, vol. 35, pp. 383–390, 2012.

[105] B. Al-Sakere *et al.*, "A study of the immunological response to tumor ablation with irreversible electroporation," *Technol. Cancer Res. Treat.*, vol. 6, no. 4, pp. 301–306, Aug. 2007.

[106] A. Ivorra *et al.*, "In vivo electrical conductivity measurements during and after tumor electroporation: Conductivity changes reflect the treatment outcome," *Phys. Med. Biol.*, vol. 54, no. 19, pp. 5949–5963, Oct. 2009.

[107] R. E. Neal 2nd *et al.*, "Treatment of breast cancer through the application of irreversible electroporation using a novel minimally invasive single needle electrode," *Breast Cancer Res. Treat.*, vol. 123, no. 1, pp. 295–301, Aug. 2010.

[108] Z. Qin *et al.*, "Irreversible electroporation: An in vivo study with dorsal skin fold chamber," *Ann. Biomed. Eng.*, vol. 41, pp. 619–629, Mar. 2013.

[109] P. A. Garcia *et al.*, "Non-thermal irreversible electroporation (N-TIRE) and adjuvant fractionated radiotherapeutic multimodal therapy for intracranial malignant glioma in a canine patient," *Technol. Cancer Res. Treat.*, vol. 10, no. 1, pp. 73–83, Feb. 2011.

[110] P. A. Garcia *et al.*, "Electrical conductivity changes during irreversible electroporation treatment of brain cancer," in *Proc. IEEE Eng. Med. Biol. Soc. Annu. Int. Conf.*, 2011, pp. 739–742.

[111] R. E. Neal 2nd *et al.*, "Successful treatment of a large soft tissue sarcoma with irreversible electroporation," *J. Clin. Oncol.*, vol. 29, no. 13, pp. e372–e377, May 2011.

[112] E. Maor *et al.*, "The effect of irreversible electroporation on blood vessels," *Technol. Cancer Res. Treat.*, vol. 6, no. 4, pp. 307–312, Aug. 2007.
[113] E. Maor *et al.*, "Non thermal irreversible electroporation: Novel technology for vascular smooth muscle cells ablation," *PLoS ONE*, vol. 4, no. 3, p. e4757, Mar. 2009.
[114] M. Phillips *et al.*, "Nonthermal irreversible electroporation for tissue decellularization," *J. Biomech. Eng.*, vol. 132, no. 9, p. 091003, Sep. 2010.
[115] M. Phillips *et al.*, "Principles of tissue engineering with nonthermal irreversible electroporation," *J. Heat Transf.*, vol. 133, no. 1, p. 011004, 2011.
[116] J. Lavee *et al.*, "A novel nonthermal energy source for surgical epicardial atrial ablation: Irreversible electroporation," in *Proc. Heart Surgery Forum*, 2007, vol. 10, pp. 162–167.
[117] J. F. Edd and R. V. Davalos, "Mathematical modeling of irreversible electroporation for treatment planning," *Technol. Cancer Res. Treat.*, vol. 6, no. 4, pp. 275–286, 2007.
[118] R. Cannon *et al.*, "Safety and early efficacy of irreversible electroporation for hepatic tumors in proximity to vital structures," *J. Surg. Oncol.*, vol. 107, no. 5, pp. 544–549, Apr. 2013.
[119] P. A. Garcia *et al.*, "A numerical investigation of the electric and thermal cell kill distributions in electroporation-based therapies in tissue," *PloS One*, vol. 9, no. 8, p. e103083, 2014.
[120] R. Goel *et al.*, "TNF-α-based accentuation in cryoinjury—Dose, delivery, and response," *Mol. Cancer Ther.*, vol. 6, no. 7, pp. 2039–2047, Jul. 2007.
[121] R. E. Neal II, "Spectrum of imaging and characteristics for liver tumors treated with irreversible electroporation," *J. Biomed. Sci. Eng.*, vol. 05, no. 12, pp. 813–818, 2012.
[122] E. W. Lee *et al.*, "Imaging guided percutaneous irreversible electroporation: ultrasound and immunohistological correlation," *Technol. Cancer Res. Treat.*, vol. 6, no. 4, pp. 287–294, Aug. 2007.
[123] L. Appelbaum *et al.*, "US findings after irreversible electroporation ablation: Radiologic-pathologic correlation," *Radiology*, vol. 262, no. 1, pp. 117–125, Jan. 2012.
[124] J. E. Coad and J. C. Bischof, "Histologic differences between cryothermic and hyperthermic therapies," *Proc. SPIE*, vol. 4954, p. 27, 2003.
[125] C. C. Rupp *et al.*, "Cryosurgical changes in the porcine kidney: Histologic analysis with thermal history correlation," *Cryobiology*, vol. 45, no. 2, pp. 167–182, 2002.
[126] N. Z. Wu *et al.*, "Measurement of material extravasation in microvascular networks using fluorescence video-microscopy," *Microvasc. Res.*, vol. 46, no. 2, pp. 231–253, Sep. 1993.
[127] K. Thomson, "Human experience with irreversible electroporation," in *Irreversible Electroporation*, B. Rubinsky, Ed. Berlin, Germany: Springer, 2010, pp. 249–254.
[128] M. Pech *et al.*, "Irreversible electroporation of renal cell carcinoma: A first-in-man phase I clinical study," *Cardiovasc. Intervent. Radiol.*, vol. 34, no. 1, pp. 132–138, 2011.
[129] K. R. Thomson *et al.*, "Investigation of the safety of irreversible electroporation in humans," *J. Vasc. Interv. Radiol.*, vol. 22, no. 5, pp. 611–621, May 2011.
[130] T. P. Kingham *et al.*, "Ablation of perivascular hepatic malignant tumors with irreversible electroporation," *J. Am. Coll. Surg.*, vol. 215, no. 3, pp. 379–387, Sep. 2012.
[131] P. Philips *et al.*, "Irreversible electroporation ablation (IRE) of unresectable soft tissue tumors: Learning curve evaluation in the first 150 patients treated," *PLoS ONE*, vol. 8, no. 11, p. e76260, Nov. 2013.
[132] S. Robert *et al.*, "Irreversible electroporation for unresectable hepatocellular carcinoma: Initial experience and review of safety and outcomes," *Technol. Cancer Res. Treat.*, vol. 12, no. 3, pp. 233–241, 2013.
[133] R. C. G. Martin II *et al.*, "Irreversible electroporation therapy in the management of locally advanced pancreatic adenocarcinoma," *J. Am. Coll. Surg.*, vol. 215, no. 3, pp. 361–369, Sep. 2012.
[134] R. E. Neal *et al.*, "In vivo characterization and numerical simulation of prostate properties for non-thermal irreversible electroporation ablation," *The Prostate*, vol. 74, no. 5, pp. 458–468, May 2014.
[135] R. C. G. Martin II *et al.*, "Irreversible electroporation in locally advanced pancreatic cancer: Potential improved overall survival," *Ann. Surg. Oncol.*, vol. 20, no. 3, pp. 443–449, Dec. 2013.
[136] H. J. Scheffer *et al.*, "Irreversible electroporation for nonthermal tumor ablation in the clinical setting: A systematic review of safety and efficacy," *J. Vasc. Interv. Radiol.*, vol. 25, no. 7, pp. 997–1011, Jul. 2014.
[137] B. Mali *et al.*, "The effect of electroporation pulses on functioning of the heart," *Med. Biol. Eng. Comput.*, vol. 46, no. 8, pp. 745–757, Aug. 2008.
[138] L. Solbiati *et al.*, "Percutaneous radio-frequency ablation of hepatic metastases from colorectal cancer: Long-term results in 117 patients," *Radiology*, vol. 221, no. 1, pp. 159–166, Oct. 2001.
[139] E. K. Abdalla *et al.*, "Recurrence and outcomes following hepatic resection, radiofrequency ablation, and combined resection/ablation for colorectal liver metastases," *Ann. Surg.*, vol. 239, no. 6, pp. 818–827, Jun. 2004.
[140] A. S. Pearson *et al.*, "Intraoperative radiofrequency ablation or cryoablation for hepatic malignancies," *Am. J. Surg.*, vol. 178, no. 6, pp. 592–598, Dec. 1999.
[141] R. Goel *et al.*, "Adjuvant approaches to enhance cryosurgery," *J. Biomech. Eng.*, vol. 131, no. 7, p. 074003, 2009.
[142] C. Daniels and B. Rubinsky, "Electrical field and temperature model of nonthermal irreversible electroporation in heterogeneous tissues," *J. Biomech. Eng.*, vol. 131, no. 7, p. 071006, Jul. 2009.
[143] C. B. Arena *et al.*, "Theoretical considerations of tissue electroporation with high-frequency bipolar pulses," *IEEE Trans. Biomed. Eng.*, vol. 58, no. 5, pp. 1474–1482, May 2011.
[144] M. Kanduser *et al.*, "Effect of surfactant polyoxyethylene glycol (C12E8) on electroporation of cell line DC3F," *Colloids Surf. Physicochem. Eng. Asp.*, vol. 214, no. 1, pp. 205–217, 2003.
[145] C. Jiang *et al.*, "An in vitro study on adjuvant enhanced irreversible electroporation," presented at the Summer Bioengineering Conf., Farjardo, PR, USA, 2012.
[146] S. N. Murthy *et al.*, "Surfactant-enhanced transdermal delivery by electroporation," *J. Controlled Release*, vol. 98, no. 2, pp. 307–315, Aug. 2004.
[147] S. N. Murthy *et al.*, "Cyclodextrin enhanced transdermal delivery of piroxicam and carboxyfluorescein by electroporation," *J. Controlled Release*, vol. 99, no. 3, pp. 393–402, Oct. 2004.
[148] G. C. Troiano *et al.*, "The effects of gramicidin on electroporation of lipid bilayers," *Biophys. J.*, vol. 76, no. 6, pp. 3150–3157, Jun. 1999.
[149] I. van Uitert *et al.*, "The influence of different membrane components on the electrical stability of bilayer lipid membranes," *Biochim. Biophys. Acta BBA Biomembr.*, vol. 1798, no. 1, pp. 21–31, Jan. 2010.
[150] J. C. Weaver *et al.*, "Heparin alters transdermal transport associated with electroporation," *Biochem. Biophys. Res. Commun.*, vol. 234, no. 3, pp. 637–640, May 1997.
[151] T. E. Zewert *et al.*, "Creation of transdermal pathways for macromolecule transport by skin electroporation and a low toxicity, pathway-enlarging molecule," *Bioelectrochem. Bioenerg.*, vol. 49, no. 1, pp. 11–20, Oct. 1999.

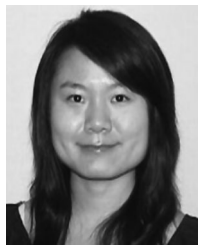

Chunlan Jiang received the B.Eng. degree from the Harbin Institute of Technology, Harbin, China, and the M.S. degree in mechanical engineering from the University of Minnesota, Minneapolis, MN, USA, where she is currently working toward the Ph.D. degree in mechanical engineering.

Since 2011, she has been a Research Assistant with the BioHeat and Mass Transfer Laboratory, University of Minnesota. Her research interests include design and preclinical testing of medical devices, irreversible electroporation, ablation therapies for cancer, cardiovascular and neural diseases, and treatment planning and enhancement.

Rafael V. Davalos (M'09) received the B.S. degree from Cornell University, Ithaca, NY, USA, and the M.S. and Ph.D. degrees from the University of California, Berkeley, CA, USA.

He is currently an Associate Professor at the Virginia Tech-Wake Forest University School of Biomedical Engineering and Sciences, Virginia Tech, Blacksburg, VA, USA. He holds Adjunct Appointments in Mechanical Engineering, Engineering Sciences and Mechanics, the Wake Forest Comprehensive Cancer Center, and the Wake Forest Institute of Regenerative Medicine. Prior to his career as a Faculty Member, he was a Principal Member of Technical Staff at Sandia National Laboratories.

John C. Bischof received the B.S. degree in bioengineering from University of California, Berkeley (UCB), CA, USA, in 1987, the M.S. degree from UCB and University of California, San Francisco, CA, in 1989, and the Ph.D. degree in mechanical engineering from UCB in 1992.

After a Postdoctoral Fellowship at Harvard in the Center for Engineering in Medicine, he joined the University of Minnesota in 1993. He is currently a Distinguished McKnight University Professor in the Departments of Mechanical and Biomedical Engineering and the inaugural Carl and Janet Kuhrmeyer Chair in Mechanical Engineering at the University of Minnesota.